

A novel octagonal slot circular compact ultrawideband antenna with detailed frequency and time-domain analysis

Satish Kumar Kannale, Nagashettappa Biradar

Department of Electronics and Communication Engineering, Bheemanna Khandre Institute of Technology, Bhalki, India

Article Info

Article history:

Received Jun 17, 2022

Revised Nov 3, 2022

Accepted Jan 11, 2023

Keywords:

Frequency and time-domain
Octagonal and trapezoidal slot
Ultrawideband

ABSTRACT

With time, the device's reliance on wireless communication and its users grows tremendously. The ultrawideband (UWB) technology offers a 7.5 GHz uncontrolled bandwidth. Because it allows for larger data rates over a short distance, UWB technology is the current and future requirement of new generation mobile networks. As a result, a novel octagonal slot circular compact UWB antenna with detailed frequency and time-domain analysis is proposed in this research. Throughout the UWB range, the hexagonal-shaped circular radiator aids in reaching better S11 parameters ($S_{11} < -10$ dB). The modified trapezoidal like partial ground plane allows for a wide bandwidth. The proposed UWB antenna operates at frequencies ranging from 3.2 to 13.1 GHz, allowing for a bandwidth of 9.9 GHz and a fractional bandwidth of 121.4%. Voltage standing wave ratio (VSWR) is seen to be in the range of 1 to 2 throughout this UWB range. Throughout the operational bandwidth, the antenna's gain ranges from 2.8 to 4.1 dB. The suggested UWB antenna has the advantages of being small, having superior impedance matching, a simple design, and having a high gain, all of which can be used to deploy the antenna for the aforementioned purposes.

This is an open access article under the [CC BY-SA](https://creativecommons.org/licenses/by-sa/4.0/) license.



Corresponding Author:

Satish Kumar Kannale

Department of Electronics and Communication Engineering, Bheemanna Khandre Institute of Technology
Bhalki, Bidar, Karnataka 585328, India

Email: ksatish.rec@gmail.com

1. INTRODUCTION

Wireless system usage has exploded in recent years, and it is now used for a variety of purposes. Mobile technology in the future will combine numerous functions into a single device, such as sharing voice, image, video, or massive amounts of data. For flawless data transmission and reception, many applications require a high data rate. To overcome this issue, the literature points to ultrawideband (UWB) systems. The distinctive properties of UWB technology, notably mobile, radar, and vehicular technologies [1]–[5], have piqued the interest of academics and industry. The antenna is one of the most important components in a UWB system, and it has the potential to degrade the overall system's performance. Short-range high-data-rate communication is possible using the unlicensed 7.5 GHz frequency spectrum, which spans the range of 3.1 to 10.6 GHz. Because effective isotropic power radiation is less than 75 nW/MHz, communication is limited to small distances [6].

Existing work in the UWB system shows a variety of monopole radiating structures, such as rectangles and circles, with various shapes carved on the radiating and ground planes [6]–[13]. The most difficult aspect of designing the UWB system is achieving impedance matching over a broader bandwidth while maintaining stable radiation characteristics. UWB antennas can be designed using a variety of methods. Research by Marchais *et al.* [14] created the UWB slot antenna. Similarly, employing an inverted-A

monopole, Suriya and Anbazhagan [15] presented a multiple-input-multiple-output (MIMO) antenna that works in the UWB spectrum. Research by Hossain *et al.* [16] proposed an UWB antenna with a bird face monopole. Research by Sanyal *et al.* [17] presented a monopole UWB antenna that might be shrunk. Research by Okas *et al.* [18] an elliptical ground plane with a notch and tapered microstrip feedline is proposed for wideband application, along with a modification to a traditional rectangular monopole antenna. Research by Okas *et al.* [18] proposes a partial monopole antenna with a circular form and an ellipse-shaped slit that minimises the lower operating frequency. V-shaped and split ring-shaped slits are used to create a UWB antenna [19]–[23].

This study shows a UWB monopole antenna with a circular structure and a feedline with an octagonal slot as a radiating plane and a modified trapezoidal like partial ground plane. This configuration offers a 121.4% impedance bandwidth extending from 3.2 to 13.1 GHz. The predicted design's physical dimension is 35.5×30 mm². The effectiveness of antenna design is evaluated using comprehensive frequency and time-domain metrics.

2. ANTENNA DESIGN

The predicted antenna fundamental frequency can be calculated as (1):

$$L_{parasiticelement} = \frac{\lambda_g}{4} \tag{1}$$

Where λ_g is the guided wavelength and is equal to.

$$\begin{aligned} \lambda_g &= \frac{\lambda_0}{\sqrt{\epsilon_{eff}}} \\ \therefore L_{parasiticelement} &= \frac{\lambda_0}{4\sqrt{\epsilon_{eff}}} \\ L_{parasiticelement} &= \frac{c}{4f_r\sqrt{\epsilon_{eff}}} \end{aligned} \tag{2}$$

Where ϵ_{eff} , f_r , c is the effective dielectric constant, resonant frequency, and speed of light.

As a radiating plane and lowered ground plane, the proposed circular-shaped UWB antenna is made up of a composite structure consisting of an octagonal slot and a modified trapezoidal ground plane. The ground and radiating plane dimensions are determined using a comprehensive parametric analysis. The proposed design calls for a FR-4 substrate with a dimension of 35.5×30 mm², as well as a microstrip transmission line for feeding. The proposed antenna is based on a traditional rectangular patch antenna with the monopole like ground plane. Focusing on impedance bandwidth curves, many iterations are carried out. The adjustment to the feedline and ground plane perturbs the identical current distribution and generates the local path, which results in a higher operating frequency. To increase impedance matching at the higher frequency of the UWB range, a 180-degree flipped trapezoidal ground with a size of (Z10×Z11×Z12×Z13×Z14) is carved on the ground plane, as depicted in Figures 1(a) and (b). The geometrical information is summarised in Table 1.

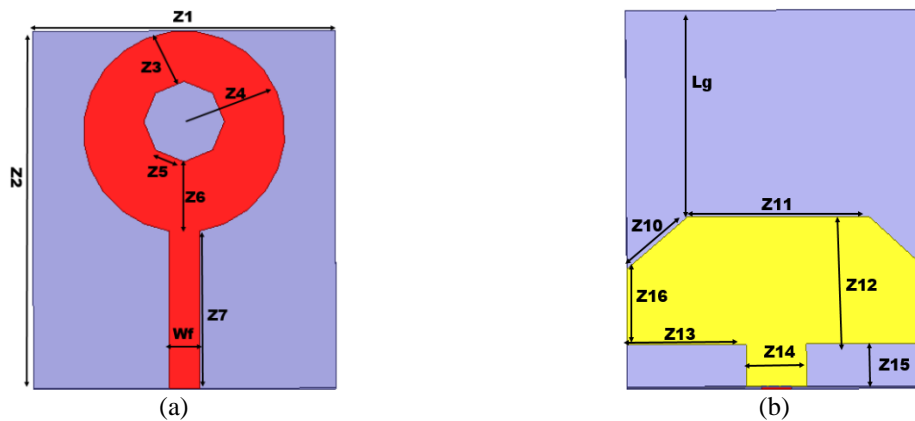


Figure 1. Projected UWB antenna (a) radiator and (b) ground plane

Table 1. Physical dimensions of the projected UWB antenna

Parameter	Dimension (mm)
Z1	30
Z2	35.5
Z3	5.2
Z4	9
Z5	3
Z6	6.7
Z7	15.6
Wf	3
Lg	19.5
Z10	7.8
Z11	18.28
Z12	12
Z13	12
Z14	6
Z15	4
Z16	7.15

In Figure 2, the current distribution is simulated and studied in order to realise the proposed UWB antenna's operation. At the operating frequencies of 3.2, 4.2, 8.5, 10.9, and 13.1 GHz, the resonance properties are investigated. Distinct portions of the antenna have different resonance routes for different operating modes, as conveyed in Figure 2. The greatest current is shown in Figure 2(a) in the lower part of the patch feed and ground, which is very active at 3.2 GHz. The greatest current is depicted in Figure 2(b) in the lower part of the patch and feed, which is very active at 4.2 GHz. The dense current is depicted in Figure 2(c) in the lower part of the patch, feedline, upper and middle half of trapezoidal ground part, which is very active at 8.5 GHz. Similarly, the greatest current is depicted in Figures 2(d) and (e) in the lower part of the patch and throughout the feed and vertical line of trapezoidal ground plane, which is very active at 10.9 and 13.1 GHz. Thus, it demonstrates that the antenna operating behavior at frequencies of of 3.2, 4.2, 8.5, 10.9, and 13.1 GHz.

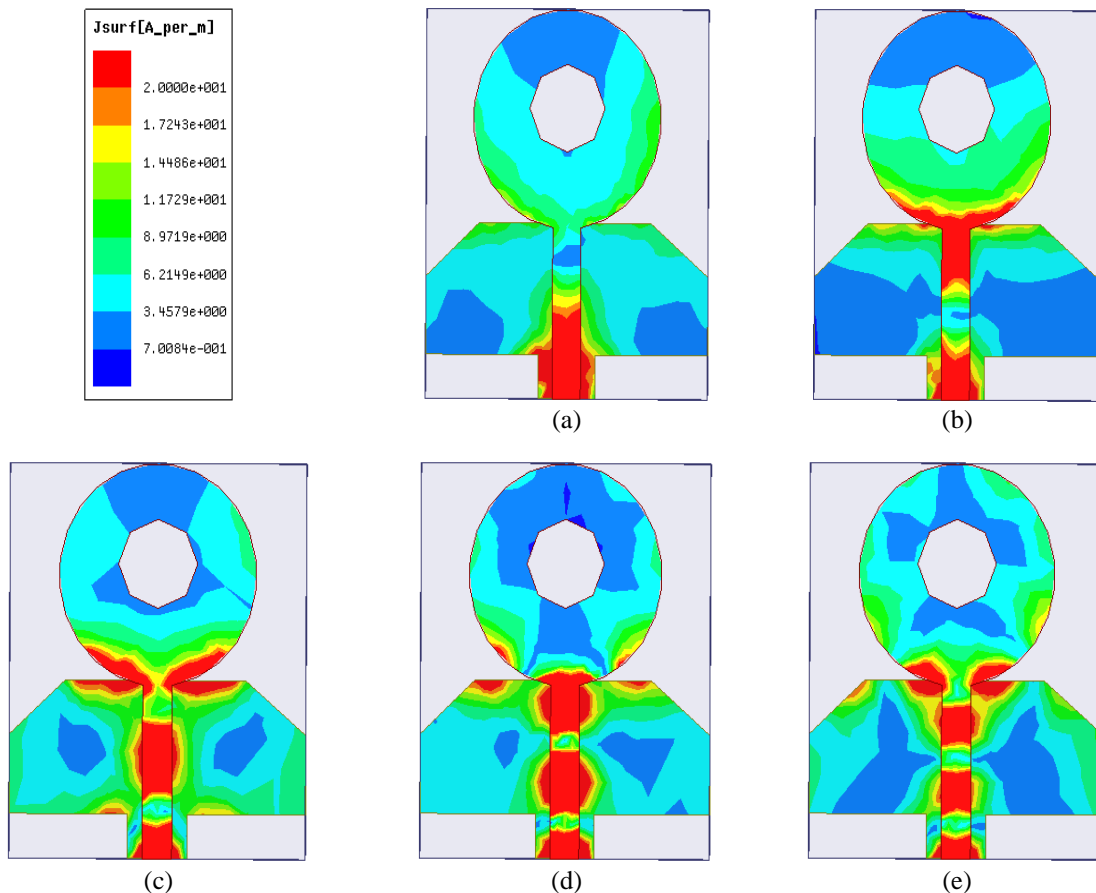


Figure 2. The current density plot of UWB at (a) 3.2, (b) 4.2, (c) 8.5, (d) 10.9, and (e) 13.1 GHz

3. PARAMETRIC ANALYSIS

3.1. Analysis of Wf

The variation in Wf was simulated and examined to investigate the effects of Wf on S11 features. Figure 3 illustrates the S11 features. The impedance matching is bad when the Wf is 4 mm and 2 mm, as can be shown. When the Wf is 3 mm, though, the effect is ideal. Thus, the chosen value of Wf is 3 mm.

3.2. Ground plane dimension Lg

The variation in Lg was simulated and evaluated in a step of 1 mm, from 15 to 17 mm, to explore the effect of the dimension Lg on the S11 features. It can be seen in Figure 4 that the Lg=16 mm model produced superior results. However, when we select Lg=15 and 16 mm the S11 deteriorates. Thus, the chosen value of Lg is 16 mm for optimum result.

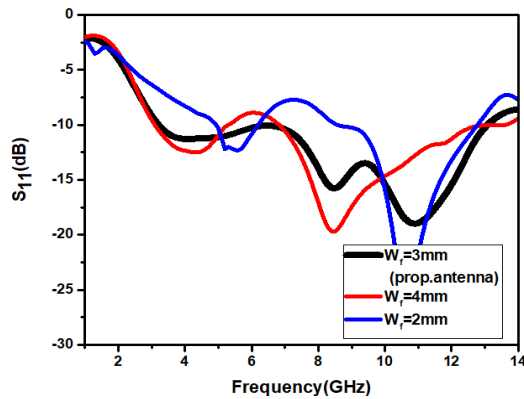


Figure 3. Feed width Wf variations

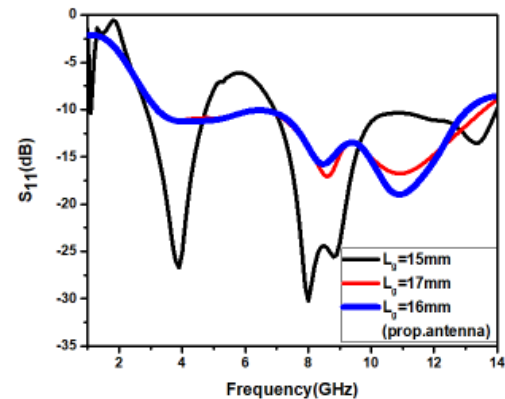


Figure 4. Ground plane dimension Lg variations

3.3. Octagonal segment variations

The variation of octagonal segment was simulated and examined to investigate the effects of it on S11 features. Figure 5 illustrates the S11 features. The impedance matching is bad when there are 10 and 6 segments, as can be shown. When the segment is 8, though, the effect is ideal for UWB.

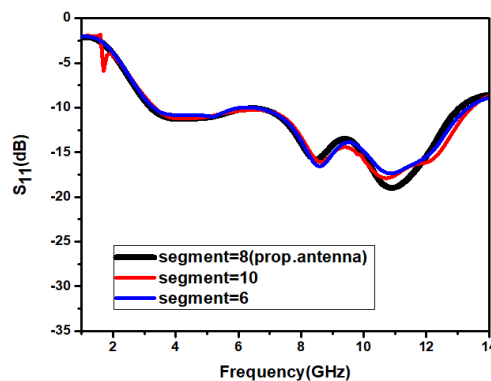


Figure 5. Octagonal segment variations

4. RESULT AND DISCUSSION

ANSYS high-frequency structure simulator (HFSS) is used to model the designed antennas. The S11 curve, radiation characteristics, and time-domain analysis are used to assess the design's efficacy. In the frequency range of 3.2 to 13.1 GHz, the S11 curve of the UWB design is substantially below -10 dB as depicted in Figure 6, and over this range the impedance curve has a real part of 50 and an imaginary part of practically zero throughout the operating frequency. Thus, a bandwidth of 9.9 GHz and a fractional bandwidth of 121.4% is exhibited by the suggested UWB antenna.

Figure 7 shows co and cross-polarization in two principle planes at operating frequencies of 3.2, 4.2, 8.5, 10.9, and 13.1 GHz for UWB. The bidirectional and omnidirectional features can be seen in the E and H planes. At 3.2, 4.2, and 8.5 GHz, the H-plane shows an omnidirectional pattern of radiation, while the E-plane shows a bidirectional pattern. It is little deviated at a frequency of 10.9 and 13.1 GHz. Thus, the the pattern in Figures 7(a)-(c) have stable pattern. Because of the multimode operation and higher harmonics, the pattern in Figures 7(d) and 7(e) becomes little unstable at higher frequencies.

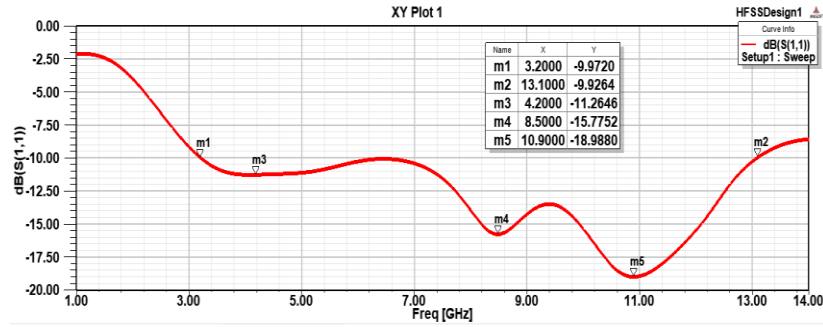


Figure 6. The UWB antenna S11 curve

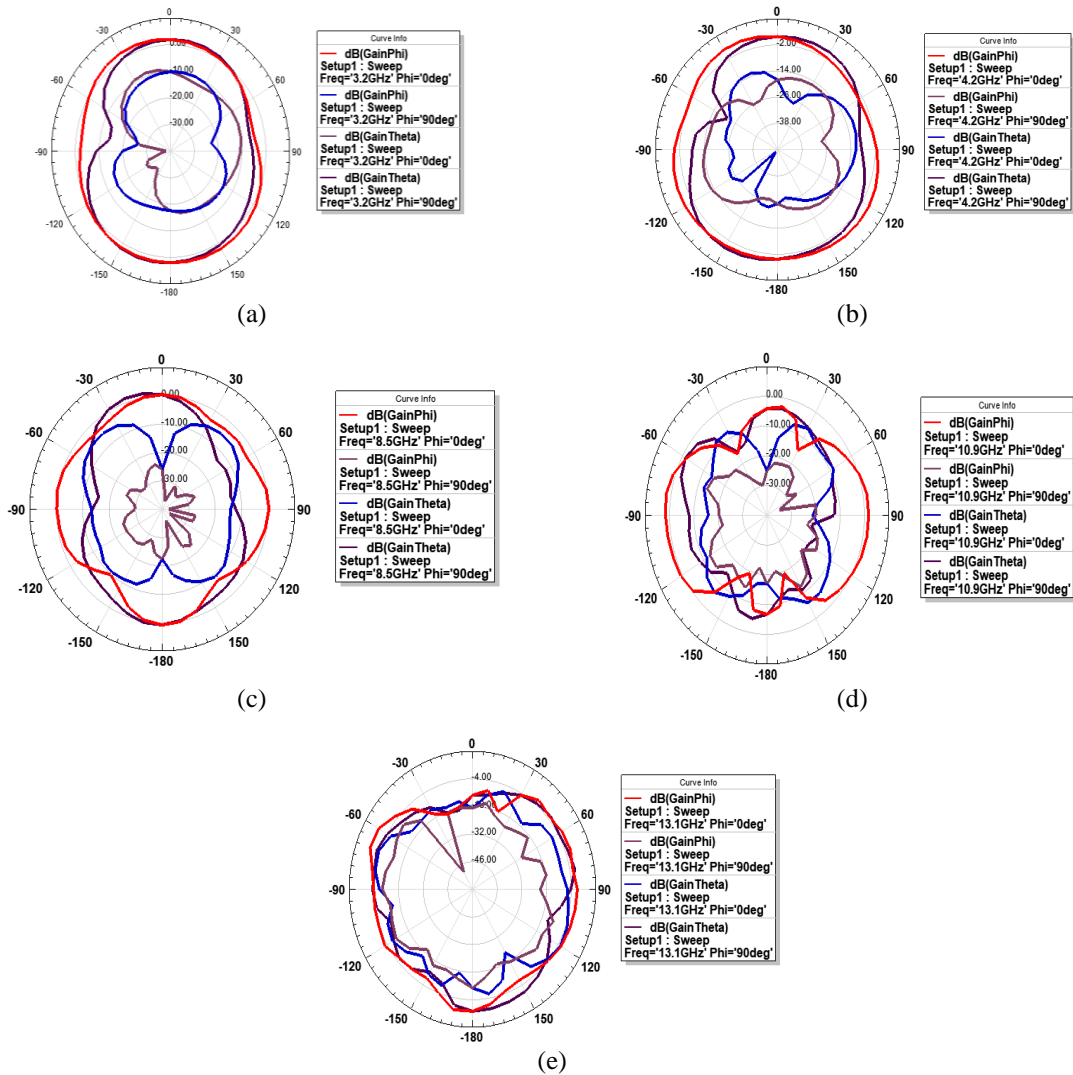


Figure 7. UWB co-polarization and cross-polarization patterns at (a) 3.2, (b) 4.2, (c) 8.5, (d) 10.9, and (e) 13.1 GHz

Furthermore, as depicted in Figure 7, the antenna's co-polarization level is high, resulting in higher repeatability of the transmitted input pulse. In addition, cross-polarization in both major planes is less than -13 dB, allowing the antenna to achieve higher electromagnetic interference performance (EMI). The maximal 3D gain of the simulated configuration is depicted in Figures 8(a)-(e). Over the range of UWB frequencies, the antenna gain ranges from 2.88 to 4.15 dB. At 3.2 GHz, there is a minimum gain of 2.88 dB, while at 13.1 GHz, there is a total gain of 4.15 dB. At a frequencies 3.2, 4.2, 8.5, 10.9, and 13.1 GHz, a total gain of 2.88, 3.22, 3.04, 4.91, and 4.15 dB is obtained respectively. The gain variation is linear in throughout the UWB, thus proving the efficacy of the the design.

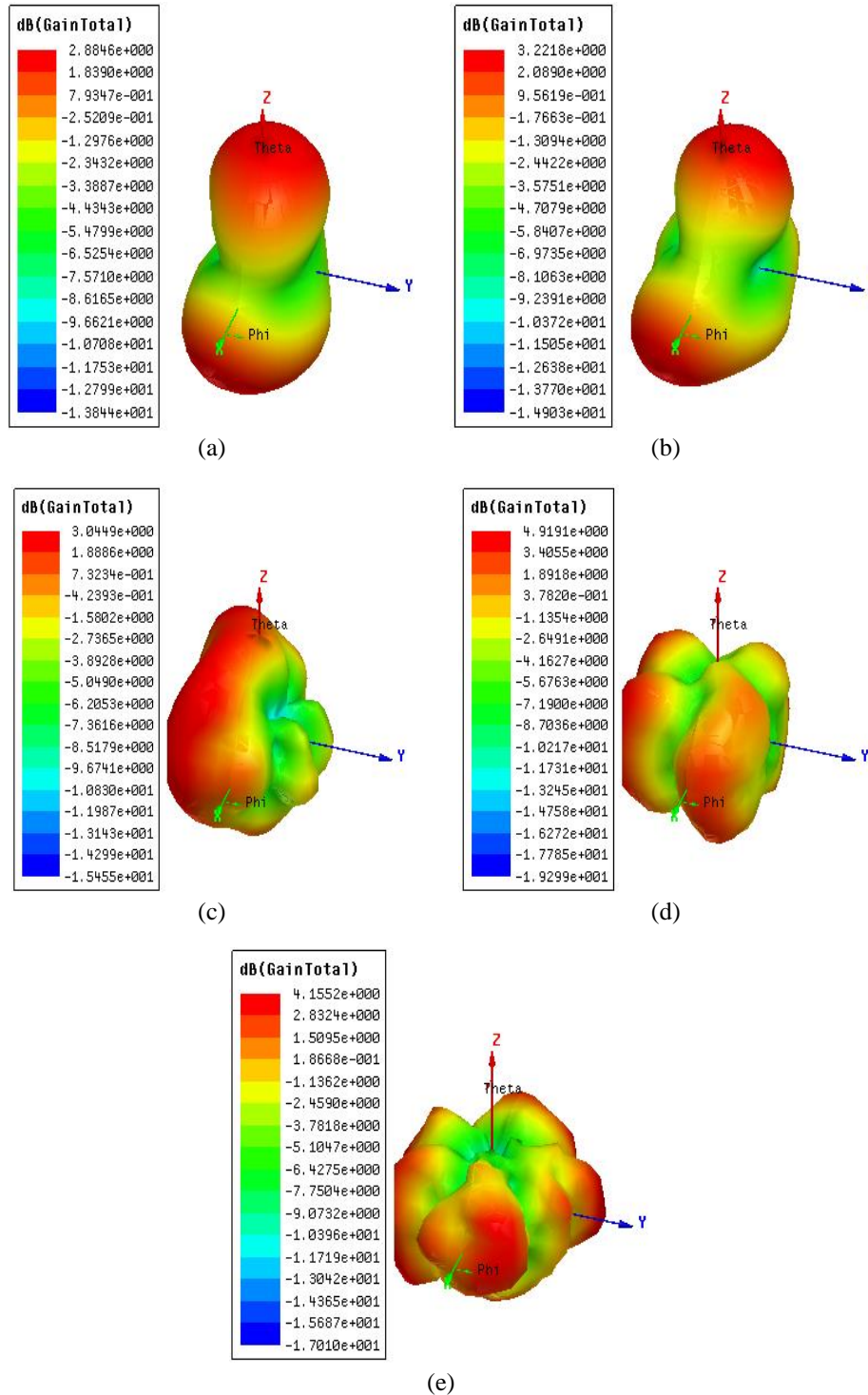


Figure 8. UWB 3D gain patterns at (a) 3.2, (b) 4.2, (c) 8.5, (d) 10.9, and (e) 13.1 GHz

5. RESULT AND DISCUSSION

UWB antennas need additional performance parameters beyond those necessary for regular antennas. For this purpose, UWB uses brief pulses to send and receive signals. Signal distortion and dispersion are possible during communication due to the obvious transmission link and distance. For the linear phase between input and output signals, the transfer function, and group latency must be investigated. Two similarly built antennas are placed side to side at a distance of 100 mm apart to study the aforementioned parameters as illustrated in Figure 9.

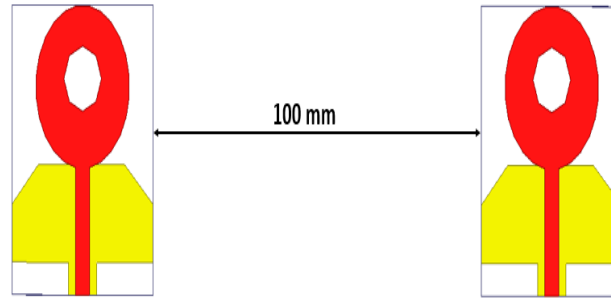


Figure 9. Time domain features are studied using a side-by-side UWB arrangement

5.1. Transfer function

Figure 10 shows the transfer function curves for UWB antenna. The amount of correlation between the elements is described by the transfer function/isolation. A can be studied in side-to-side arrangements, the UWB antennas have isolation values of less than -20 dB across the antenna's operational frequency. These figures show that the antenna has a negligible effect on correlation.

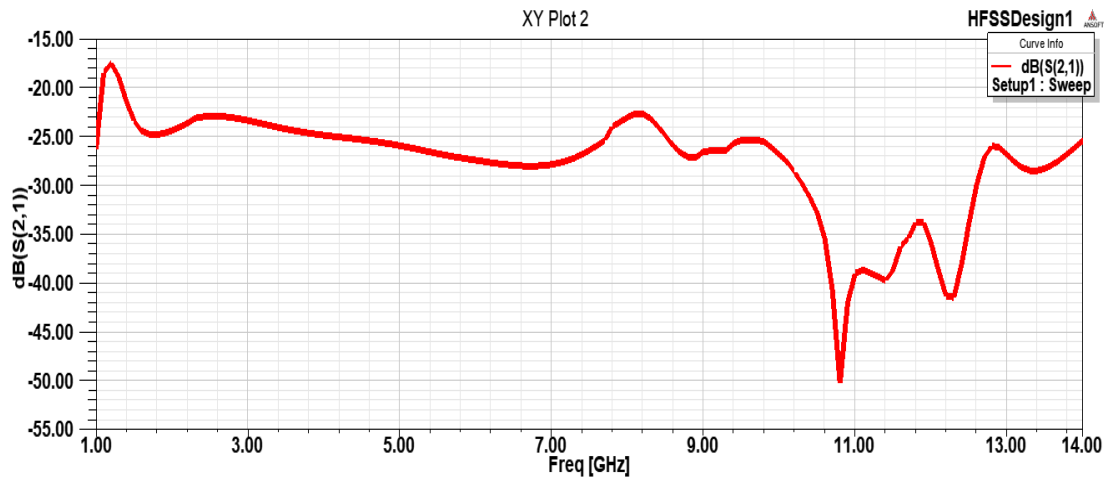


Figure 10. Transfer function of the UWB antenna

5.2. Group delay

The negative derivative of phase variation in accordance with the angular frequency is used to determine group delay. The signal is subjected to amplitude and phase disturbances as it travels. There could be multiple frequency components in the input signal. For such signals, group delay denotes the system's phase linearity and is defined by (3) [24], [25]. A group delay of less than 1 ns is considered acceptable. The group delay of the projected antennas is less than 1 ns in side to side configurations depicted in Figure 11.

$$\tau_g(\omega) = -\frac{d\varphi(\omega)}{d\omega} \quad (3)$$

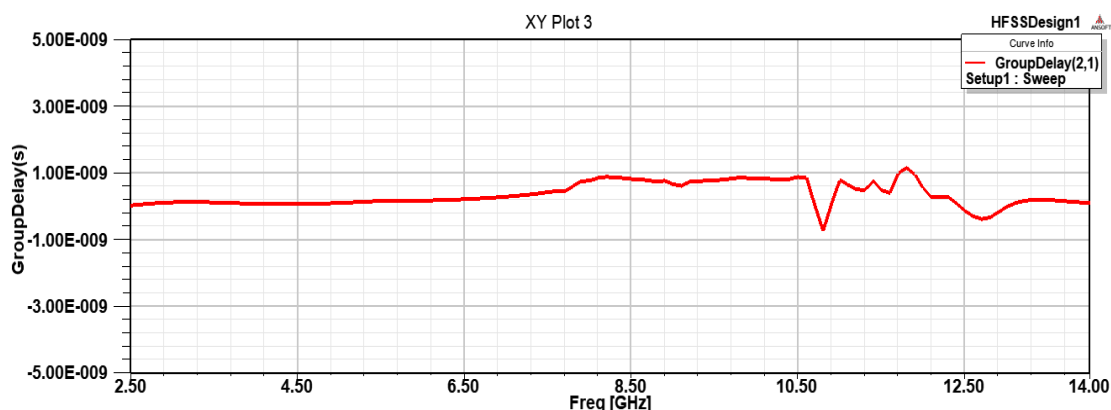


Figure 11. The UWB antenna's group delay

6. CONCLUSION

In this study, a compact circular-shaped octagonal slot UWB antenna is presented. The antenna's dimensions are 35.5×30 mm². The proposed UWB antenna operates at frequencies ranging from 3.2 to 13.1 GHz, allowing for a bandwidth of 9.9 GHz and a fractional bandwidth of 121.4%. The modified trapezoidal shaped partial ground plane helps in exhibiting broad bandwidth. Throughout the operational bandwidth, the antenna's gain ranges from 2.88 to 4.15 dB. Time-domain measures like as isolation, and group latency are explored in the predicted designs. The suggested UWB antenna has the advantages of being small, having superior impedance matching, simple design, and having a high gain. The results of the studies show that it is suitable for wireless communication applications.




REFERENCES

- [1] P. Kumar, M. M. M. Pai, and T. Ali, "Ultrawideband antenna in wireless communication: A review and current state of the art," *Telecommunications and Radio Engineering*, vol. 79, no. 11, pp. 929–942, 2020, doi: 10.1615/TelecomRadEng.v79.i11.20.
- [2] P. Kumar, M. M. M. Pai, and T. Ali, "Design and analysis of multiple antenna structures for ultrawide bandwidth," *Telecommunications and Radio Engineering*, vol. 80, no. 6, pp. 41–53, 2021, doi: 10.1615/TelecomRadEng.2021038819.
- [3] K. Yan, Z. Xia, S. Wu, X. Liu, and G. Fang, "Through-floor vital sign imaging for trapped persons based on optimized 2-D UWB life-detection radar deployment," *IEEE Antennas and Wireless Propagation Letters*, vol. 21, no. 1, pp. 39–43, Jan. 2022, doi: 10.1109/LAWP.2021.3116610.
- [4] Y. Song, T. Jin, Y. Dai, and X. Zhou, "Efficient through-wall human pose reconstruction using UWB MIMO radar," *IEEE Antennas and Wireless Propagation Letters*, vol. 21, no. 3, pp. 571–575, Mar. 2022, doi: 10.1109/LAWP.2021.3138512.
- [5] D. Potti *et al.*, "A novel optically transparent UWB antenna for automotive MIMO communications," *IEEE Transactions on Antennas and Propagation*, vol. 69, no. 7, pp. 3821–3828, Jul. 2021, doi: 10.1109/TAP.2020.3044383.
- [6] P. Kumar, T. Ali, and M. M. M. Pai, "Electromagnetic metamaterials: A new paradigm of antenna design," *IEEE Access*, vol. 9, pp. 18722–18751, 2021, doi: 10.1109/ACCESS.2021.3053100.
- [7] P. Kumar, M. M. M. Pai, and T. Ali, "Metamaterials: New aspects in antenna design," *Telecommunications and Radio Engineering*, vol. 79, no. 16, pp. 1467–1478, 2020, doi: 10.1615/TelecomRadEng.v79.i16.50.
- [8] G. Kumar and R. Kumar, "A survey on planar ultra-wideband antennas with band notch characteristics: Principle, design, and applications," *AEU-International Journal of Electronics and Communications*, vol. 109, pp. 76–98, Sep. 2019, doi: 10.1016/j.aeue.2019.07.004.
- [9] N. N. Kumar *et al.*, "A slotted UWB monopole antenna with truncated ground plane for breast cancer detection," *Alexandria Engineering Journal*, vol. 59, no. 5, pp. 3767–3780, Oct. 2020, doi: 10.1016/j.aej.2020.06.034.
- [10] W. Balani, M. Sarvagya, A. Samasgikar, T. Ali, and P. Kumar, "Design and analysis of super wideband antenna for microwave applications," *Sensors*, vol. 21, no. 2, pp. 1–29, Jan. 2021, doi: 10.3390/s21020477.
- [11] O. P. Kumar, P. Kumar, T. Ali, P. Kumar, and S. Vincent, "Ultrawideband antennas: Growth and evolution," *Micromachines*, vol. 13, no. 1, pp. 1–45, Dec. 2021, doi: 10.3390/mi13010060.
- [12] M. J. Ammann and Z. N. Chen, "Wideband monopole antennas for multi-band wireless systems," *IEEE Antennas and Propagation Magazine*, vol. 45, no. 2, pp. 146–150, Apr. 2003, doi: 10.1109/MAP.2003.1203133.
- [13] Y.-M. Pan, K. W. Leung, and K. Lu, "Compact quasi-isotropic dielectric resonator antenna with small ground plane," *IEEE Transactions on Antennas and Propagation*, vol. 62, no. 2, pp. 577–585, Feb. 2014, doi: 10.1109/TAP.2013.2292082.
- [14] C. Marchais, G. le Ray, and A. Sharaiha, "Stripline slot antenna for UWB communications," *IEEE Antennas and Wireless Propagation Letters*, vol. 5, no. 1, pp. 319–322, 2006, doi: 10.1109/LAWP.2006.878894.
- [15] I. Suriya and R. Anbazhagan, "Inverted-A based UWB MIMO antenna with triple-band notch and improved isolation for WBAN applications," *AEU-International Journal of Electronics and Communications*, vol. 99, pp. 25–33, Feb. 2019, doi: 10.1016/j.aeue.2018.11.030.
- [16] M. J. Hossain, M. R. I. Faruque, M. M. Islam, M. T. Islam, and M. A. Rahman, "Bird face microstrip printed monopole antenna design for ultra wide band applications," *Frequenz*, vol. 70, no. 11–12, pp. 473–478, Jan. 2016, doi: 10.1515/freq-2016-0113.
- [17] P. Sanyal, P. Sarkar, and S. K. Chowdhury, "Miniaturized band notched UWB antenna with improved fidelity factor and pattern stability," *Radioengineering*, vol. 27, no. 1, pp. 39–46, Apr. 2018, doi: 10.13164/re.2018.0039.
- [18] P. Okas, A. Sharma, and R. K. Gangwar, "Circular base loaded modified rectangular monopole radiator for super wideband




- application," *Microwave and Optical Technology Letters*, vol. 59, no. 10, pp. 2421–2428, Oct. 2017, doi: 10.1002/mop.30757.
- [19] H. Bong, M. Jeong, N. Hussain, S. Rhee, S. Gil, and N. Kim, "Design of an UWB antenna with two slits for 5G/WLAN-notched bands," *Microwave and Optical Technology Letters*, vol. 61, no. 5, pp. 1295–1300, May 2019, doi: 10.1002/mop.31670.
- [20] P. Kumar *et al.*, "A compact quad-port UWB MIMO antenna with improved isolation using a novel mesh-like decoupling structure and unique DGS," *IEEE Transactions on Circuits and Systems II: Express Briefs*, pp. 1–1, 2022, doi: 10.1109/TCSII.2022.3220542.
- [21] M. Pallavi, P. Kumar, T. Ali, and S. B. Shenoy, "Modeling of a negative refractive index metamaterial unit-cell and array for aircraft surveillance applications," *IEEE Access*, vol. 10, pp. 99790–99812, 2022, doi: 10.1109/ACCESS.2022.3206358.
- [22] H. Islam *et al.*, "Bandstop filter decoupling technique for miniaturized reconfigurable MIMO antenna," *IEEE Access*, vol. 10, pp. 19060–19071, 2022, doi: 10.1109/ACCESS.2022.3150348.
- [23] P. Kumar *et al.*, "Design of a six-port compact UWB MIMO antenna with a distinctive DGS for improved isolation," *IEEE Access*, vol. 10, pp. 112964–112974, 2022, doi: 10.1109/ACCESS.2022.3216889.
- [24] P. Kumar, T. Ali, and M. M. Pai, "A compact highly isolated two-and four-port ultrawideband Multiple Input and Multiple Output antenna with Wireless LAN and X-band notch characteristics based on Defected Ground Structure," *International Journal of Communication Systems*, vol. 35, no. 17, pp. e5331, 2022, doi: 10.1002/dac.5331.
- [25] P. Kumar *et al.*, "A Compact Quad-Port UWB MIMO Antenna with Improved Isolation Using a Novel Mesh-Like Decoupling Structure and Unique DGS," in *IEEE Transactions on Circuits and Systems II: Express Briefs*, 2022, doi: 10.1109/TCSII.2022.3220542.

BIOGRAPHIES OF AUTHORS



Satish Kumar Kannale    received the Engineer degree in Electronics and Instrumentation Engineering from Gulbarga university Karnataka in 1999, and M.Tech (Microwave and millimeter waves) in Electronics and Communication Department from MANIT Bhupal Madhya pradesh in 2007. Currently he is pursuing Ph.D. in Electronics and Communication Engineering from Visveswaraya Technological university Belagavi Karnataka. His research interests include antenna design, wireless communication and microwave communication. He can be contacted at email: ksatish.rec@gmail.com.



Dr. Nagashettappa Biradar    acquired his BE (E&CE) and M.Tech (IE) degrees from Gulbarga University, Gulbarga and VTU, Belgaum in 1998 and 2003. He received his Ph.D. from IIT Roorkee India. Currently he is working as a Principal and Academic Senate member at Bheemanna Khandre Institute of Technology, Bhalki and VTU Belgavi Karnataka respectively. He is Guiding for seven Ph.D. Research Scholars of Vishveswaraya Technological University. Biradar has received several grants from Dept. of IT and BT, GoK and VGST Karnataka. His areas of interest are Antenna design, assessment of aortic regurgitation, denoising, and segmentation of echocardiographic images. He can be contacted at email: nmbiradar@gmail.com.